

Collision-Induced Decomposition of Multiatomic Ions

Gregory M. Neumann, Margaret M. Sheil, and Peter J. Derrick

School of Chemistry, University of New South Wales, PO Box 1, Kensington, NSW 2033, Australia

Z. Naturforsch. **39a**, 584–592 (1984); received February 24, 1984

The dependence upon ion mass of the loss of translational energy suffered by an ion with kiloelectron volt energy as a result of collision with helium has been investigated over the mass range 400 u to 1600 u. At masses below about 1500 u and an incident ion energy of 8 keV, there is forward-scattering in the centre-of-mass frame; at mass 1620 u at the same energy, there is back-scattering in the centre-of-mass frame. The uptake of internal energy by an ion is at a maximum in the region in which the change from forward-scattering to back-scattering occurs.

1. Introduction

The dynamics of collisions between atoms and macromolecules have become accessible to detailed study, through the development of techniques for producing beams of macromolecular or, as they will be called here, multiatomic ions [1–5]. The term “multiatomic” is used to mean more than 10^2 atoms. In the experiments reported here, beams of ions, formed from the peptide bombesin and other peptides and with translational energies in the kiloelectronvolt range, have been passed through inert gases, in most cases helium, at low pressures. The peptide ions are excited, and fragment to produce, what are referred to as, collision-induced decomposition (CID) spectra [6, 7]. The translational energies of fragment ions making up CID spectra have been measured, and used to calculate the translational energy losses suffered by the parent ions as a result of collision. The translational energy lost by a parent ion provides information on the internal energy taken up by that ion as a result of collision. The findings reported here appear not to be restricted to peptide ions; similar observations have been made with ions formed from various synthetic organic polymers [8].

Consider a collision between an ion $(I)^+$ and an atom A with masses m_i and m_a respectively. Let the translational energy of $(I)^+$ prior to collision be E_i , and let A be at rest prior to collision. It follows from the laws of conservation of energy and linear momentum that the internal energy Q taken up by the ion $(I)^+$ as a result of collision with A is related by the expression (1) to the translational energy ΔE_i lost by

$(I)^+$ and the angle θ_i through which $(I)^+$ is scattered. In this paper, it will be assumed that θ_i is small and can be set to zero.

$$Q = [(m_i + m_a) \Delta E_i / m_a] - [(2 m_i E_i / m_a) (1 - [(E_i - \Delta E_i) / E_i]^{1/2} \cos \theta_i)] \quad (1)$$

This assumption has been justified elsewhere [9]; additional evidence is presented below. The translational energy ΔE_i lost by $(I)^+$ is related to the internal energy Q taken up by $(I)^+$ through the expression

$$\Delta E_i = Q + \Delta E_a, \quad (2)$$

where ΔE_a is the translational energy imparted to A as a result of collision.

The objective of this study was to investigate how the uptake of internal energy Q varied with the size of the incident ion, making use of protonated bombesin $(M+H)^+$ which has a molecular mass of 1619.8 u and consists of 225 atoms. It was known [9] already that over the range of incident ion masses 400 u to 1200 u, the uptake of internal energy Q at what is known as the “optimum collision pressure” (see below) rose with mass in an approximately linear fashion. Given this linear dependence, the region just above mass 1200 was expected to be of interest because the energy uptake Q would begin to approach the collision energy in the centre-of-mass frame $E_{C.O.M.}$, which constitutes the maximum available for conversion into internal energy.

2. Experimental

All measurements were carried out on an unusually large double-focussing mass spectrometer,

Reprint requests to Prof. Dr. P. J. Derrick, School of Chemistry, University of New South Wales, PO Box 1, Kensington/NSW 2033, Australia.

0340-4811 / 84 / 0600-0584 \$ 01.3 0/0. – Please order a reprint rather than making your own copy.



Dieses Werk wurde im Jahr 2013 vom Verlag Zeitschrift für Naturforschung in Zusammenarbeit mit der Max-Planck-Gesellschaft zur Förderung der Wissenschaften e.V. digitalisiert und unter folgender Lizenz veröffentlicht: Creative Commons Namensnennung-Keine Bearbeitung 3.0 Deutschland Lizenz.

Zum 01.01.2015 ist eine Anpassung der Lizenzbedingungen (Entfall der Creative Commons Lizenzbedingung „Keine Bearbeitung“) beabsichtigt, um eine Nachnutzung auch im Rahmen zukünftiger wissenschaftlicher Nutzungsformen zu ermöglichen.

This work has been digitalized and published in 2013 by Verlag Zeitschrift für Naturforschung in cooperation with the Max Planck Society for the Advancement of Science under a Creative Commons Attribution-NoDerivs 3.0 Germany License.

On 01.01.2015 it is planned to change the License Conditions (the removal of the Creative Commons License condition “no derivative works”). This is to allow reuse in the area of future scientific usage.

which had a mass range of greater than 8000 u for singly-charged ions at an ion energy of 8 keV. This mass spectrometer, which consists of an 80 cm radius magnetic sector followed by a 100 cm radius electric sector, has been described previously [3]. A 1 cm long collision cell was fitted at the focal point between the magnetic and electric sectors. The magnetic analyser was in effect used to select the mass m_i of the multiatomic ion entering the collision cell, and the electric sector was used to measure the translational energies of the ions emerging from the collision cell [5, 6].

Ions were generated by field desorption from activated 10 μm tungsten wires, conditioned according to a variation of the high temperature activation method of Beckey *et al.* [10]. Sample material was applied to the microneedle-covered portion of the emitter wire from a mildly concentrated (nM) droplet of solution supported on a glass slide, into which droplet the emitter wire would be dipped. Excess solvent (dimethylformamide or water) was removed by complete evaporation of the droplet, leaving a uniform deposit of 0.1–1 μg of sample on the emitter.

Field desorption was carried out with a positive potential of 8 kV applied between the emitter and a cathode 2 mm away. The sample was heated by a direct current, through the emitter wire, of 10–20 mA. This was supplied, under manual control by a constant current power supply floating at the emitter potential.

Normal mass spectra (from magnetic field scans at fixed electric sector potential) were recorded using a half-height resolution of 2000 or higher. Perfluorotributylamine and polypropylene glycol [11] were employed for mass calibration.

Total ion currents of the order of nanoamperes (nA) could be generated from the peptide bombesin for periods of one hour or more. Total ion currents of the order of tens of nA could be maintained for shorter periods of time. All CID spectra were recorded at the “optimum collision pressure”, i.e. the pressure required to maximise fragment ion intensities. At the optimum collision pressure, the parent beam would be reduced to 30–40% of the incident beam intensity. Collision gas pressures were determined from measurements of the gas pressure outside the collision cell, as indicated by an ion gauge and by direct measurement using a McLeod gauge.

The translational energy loss ΔE_i suffered by an incident ion was obtained through consideration of the precise positions of the peaks in its CID spectrum. A mass scale would be set up for the CID spectrum [12], without allowance for the translational energy loss ΔE_i [9]. Peaks would then appear to be shifted from their “true” positions by an amount Δm_f , which would be proportional to the mass m_f of the fragment ion which the peak represented [12]. By “true position” is meant the assigned mass, as discussed in this paper in the case of bombesin. The shift Δm_f would be measured for as many peaks as possible in any given spectrum, and the average mass-normalised peak shift $\Delta m_f/m_f$ would be calculated. This shift is related directly to the translational energy ΔE_i lost by the incident ion [12].

3. Results

Collision cross-sections

It has been reported earlier [9] that the optimum collision pressure, defined as the pressure at which fragment peak intensities in the CID spectrum are a maximum, is inversely proportional to incident ion mass m_i in the mass range 400 to 1200 u. We have determined the optimum collision pressures for singly-charged incident ions of mass 1348 u ($(M+H)^+$ from substance P [15]), 1414 u ($(2M+H)^+$ from eldoisin-related peptide [9]) and 1620 u ($(M+H)^+$ from bombesin (see below)) at an incident ion energy of 8 keV, and found that the relationship holds at these higher masses. In Fig. 1, an absolute

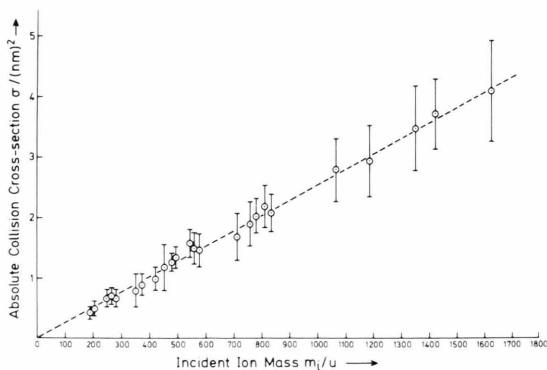


Fig. 1. Dependence of absolute collision cross-section σ upon incident ion mass m_i . Helium collision gas. Incident ion energy 8 keV in all cases.

collision cross-section σ is plotted against incident mass m_i . These cross-sections have been calculated from the optimum collision pressures determined in this and the earlier study [9], by means of the expression

$$\sigma = (kT)/(Pl), \quad (3)$$

where P is the optimum collision pressure and l the collision cell path length (1 cm). The expression (3) is obtained from the ideal gas law $PV = nkT$, on the basis that the number n of gas atoms in the volume V swept out by the incident ion while traversing the cell is one (see discussion). It can be seen (Fig. 1) that the absolute collision-cross section is approximately 4 nm^2 at 1620 u . Dawson *et al.* [13, 14] have reported a linear variation of absolute cross-section with incident ion mass in the mass range below 200 u . Their cross-sections would fall on a linear extrapolation of the plot of σ vs. m_i in Fig. 1; their collision energies in the centre-of-mass frame were comparable to those used here.

Over the range of ion masses investigated here and earlier [9], the optimum collision pressure was found to correspond to a reduction of the incident ion beam to 30–40% of its original intensity. This figure of 30–40% was not altered by varying the incident ion energy over the range 4 keV – 14 keV . The figure was also not sensitive to collision gas, being the same with argon as with helium. For $(M+H)^+$ m/z 1620 from bombesin, the magnitude of the optimum collision pressure was the same with argon as with helium.

Collision-induced decomposition (CID) spectra of bombesin

The significance to the present study of the CID spectra of the pseudomolecular ion $(M+H)^+$ and other ions from the peptide bombesin lies with the information they contain concerning translational energy loss ΔE_i as a result of collision. The ions from the field desorption (FD) mass spectrum of bombesin (Fig. 2) which have been employed as incident ions are m/z 583, m/z 680, m/z 810.4 and m/z 1619.8. Bombesin has the formula H-pGlu-Gln-Arg-Leu-Gly-Asn-Gln-Trp-Ala-Val-Gly-His-Leu-Met-NH₂, using conventional biochemical symbols, and its molecular mass M is 1618.8 u . The strongest peak in the FD mass spectrum at m/z 810.4, corresponds to the $(M+2H)^{2+}$ ion; m/z 1619.8 cor-

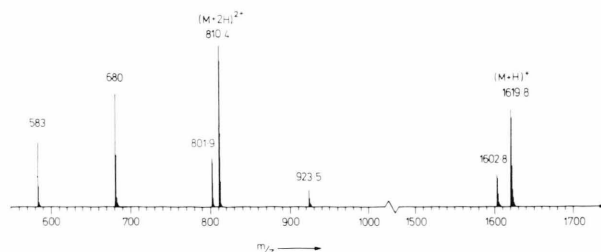


Fig. 2. Field desorption mass spectrum of the peptide bombesin. Emitter heating current 17 mA .

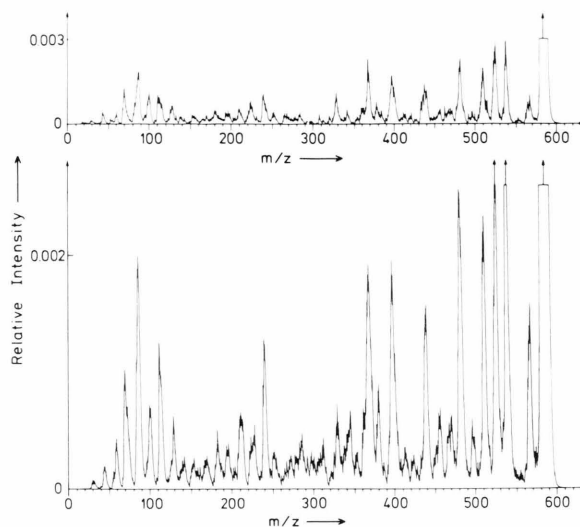


Fig. 3. CID-spectrum of the m/z 583 fragment ion produced during field desorption of bombesin. Helium collision gas pressure: 0.3 Pa .

responds to the $(M+H)^+$ ion. The intense peaks at m/z 583 and m/z 680 are assigned to the N-terminal fragment ions $(\text{H-pGlu-Gln-Arg-Leu-Gly-NH}_2 + \text{H})^+$ and $(\text{H-pGlu-Gln-Arg-Leu-Gly-Asn})^+$ respectively. The terms “N-terminal” and “C-terminal” will be used to describe fragment ions incorporating the N-terminus and C-terminus respectively of a peptide [15]. If the fragment ion corresponds to rupture of a peptide bond, the more specific terms “N-sequence ion” and “C-sequence ion” will be used. A numeral inserted after the “N” or “C” will indicate which peptide bond has broken, counting the peptide bonds of a particular molecule from the N-terminus in all cases. Thus $(\text{H-pGlu-Gln-Arg-Leu-Gly-Asn})^+$ is the “N-6 sequence ion”.

The CID spectrum of the m/z 583 ion, recorded at two different sensitivities, is shown in Figure 3,

The collision gas was helium. The majority of the peaks at high masses correspond to ions formed by loss of part or all of a side-chain (the arginine side-chain in particular) or to loss of a small neutral fragment. The strong peaks at m/z 526 and m/z 483 are assigned to loss of the leucine and arginine side-chains respectively, whilst the strong peak at m/z 511 could be assigned to loss of the glutamine side-chain or to loss of part of the arginine side-chain. The peaks at m/z 568 and m/z 566 are attributed to loss of CH_3 and NH_3 respectively. Many of the peaks at low masses in the spectrum correspond to charged fragments originating from the arginine side-chain and characteristic of that amino acid [9, 15]. Peaks due to N-sequence ions appear to be present at m/z 112, m/z 240, m/z 396 and m/z 509 (overlapping with m/z 511). Strong "satellite" peaks 28 u lower in mass accompany each of the N-sequence peaks. Weak peaks due to C-sequence ions [16] appear to be present at m/z 472 and m/z 344. In the CID spectrum of the m/z 583 ion (Fig. 3), the average mass-normalised peak shift $\Delta m_f/m_f$ is $(1.5 \times 10^{-3}) \pm (0.4 \times 10^{-3})$. This represents a translational energy loss ΔE_i for m/z 583 of 12 ± 3 eV and an internal energy uptake Q of 11.5 ± 3 eV (using expression (1) with $\theta_i = 0$).

The CID spectrum (Fig. 4) of the m/z 680 fragment of bombesin, obtained using helium as the collision gas, displays a number of close similarities to the CID spectrum of the m/z 583 fragment (Fig. 3). Below m/z 390 the two spectra are essentially identical, whilst at the high mass end of each spectrum, fragment peaks correspond to the same mass losses and exhibit similar patterns of intensity. In particular, the three strong peaks in each spectrum corresponding to loss of 72 u, 57 u and 44 u respectively from the parent ion are attributed, respectively, to loss of the glutamine side-chain or part of the arginine side-chain, loss of the leucine

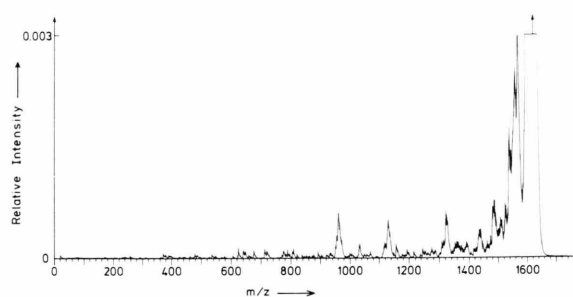


Fig. 5. CID spectrum of the $(\text{M}+\text{H})^+$ ion m/z 1619.8 of bombesin. Helium collision gas pressure: 0.1 Pa.

side-chain, and loss of the C-terminal formamido group or formamidine from the arginine side-chain. The major difference between the two spectra is that the N-3 and N-4 sequence peaks (m/z 396 and m/z 509) in the m/z 680 spectrum (Fig. 4) are considerably weaker than the same (strong) peaks in the m/z 583 spectrum (Fig. 3). The N-5 sequence peak (m/z 566) in the m/z 680 spectrum is also of low relative intensity. For the CID spectrum of the m/z 680 ion (Fig. 4), the average mass-normalized peak shift $\Delta m_f/m_f$ is $(1.7 \times 10^{-3}) \pm (0.4 \times 10^{-3})$. This represents a parent translational energy loss ΔE_i of 14 ± 3 eV and an internal energy uptake Q of 13 ± 3 eV.

The CID spectrum of the $(\text{M}+\text{H})^+$ ion of bombesin (m/z 1619.8) using helium collision gas and 8 keV incident ion energy is shown in Fig. 5. The three strongest peaks in the spectrum are assigned to the same C-terminal and side-chain losses as the three strong high mass fragment peaks in the CID spectra of the m/z 583 and m/z 680 fragments. Several of the other fragment peaks also appear to be due to side-chain losses: loss of the tryptophan side-chain (130 u), loss of the arginine side-chain (100 u) and loss of part of the arginine side-chain (86 u). The remaining peaks in the spectrum are each assigned to an N-terminal fragment from which CO is missing. The assigned masses are 966 u, 1038 u, 1137 u, 1331 u and 1444 u. The average mass-normalised peak shift $\Delta m_f/m_f$ is $(6.2 \times 10^{-3}) \pm (0.9 \times 10^{-3})$, which implies a translational energy loss ΔE_i of 50 ± 7 eV and an internal energy uptake Q of 18.5 ± 2 eV. At 20 keV incident ion energy, the translational energy loss ΔE_i of $(\text{M}+\text{H})^+$ m/z 1620 was much lower, however the internal energy uptake Q ($18.7 \text{ eV} \pm 3 \text{ eV}$) was the same as at 8 keV.

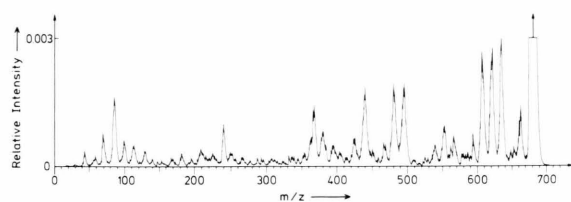


Fig. 4. CID spectrum of the m/z 680 fragment ion produced during field desorption of bombesin. Helium collision gas pressure: 0.2 Pa.

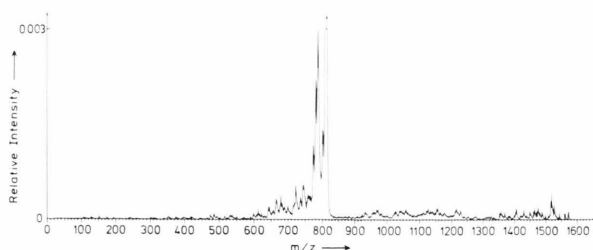


Fig. 6. CID spectrum of the $(M+2H)^{2+}$ ion, m/z 810.4 of bombesin. Helium collision gas pressure: 0.1 Pa.

The CID spectrum of the $(M+2H)^{2+}$ ion of bombesin using helium collision gas is shown in Fig. 6. The region of the spectrum above the parent peak (m/z 810.4) contains numerous poorly resolved peaks representing singly-charged fragment ions. The region of the spectrum below the parent peak bears a strong resemblance to the CID spectrum of the $(M+H)^+$ ion (Fig. 5). The three strong peaks adjacent to each other in the $(M+2H)^{2+}$ spectrum are attributed to the same C-terminal and side-chain losses are their counterparts in the $(M+H)^+$ spectrum. There is a fourth strong peak in the $(M+2H)^{2+}$ spectrum, immediately adjacent to the parent peak, the counterpart of which cannot be distinguished in the $(M+H)^+$ spectrum. The $(M+H)^+$ parent peak is considerably broader than the $(M+2H)^{2+}$ parent peak, and obscures the region where such an additional peak would fall. The additional peak in the $(M+2H)^{2+}$ spectrum does, however, have analogs in the CID spectra of the m/z 583 and m/z 680 fragments of bombesin (Figs. 3 and 4 respectively). In each of those spectra the analogous peak, which is of comparable relative intensity to the peak in the $(M+2H)^{2+}$ spectrum, is attributed to loss of CH_3 from the leucine side-chain. Fragment peaks in the $(M+2H)^{2+}$ spectrum are shifted by an average amount corresponding to a parent translational energy loss ΔE_i of $25 \text{ eV} \pm 15 \text{ eV}$. The large uncertainty in this estimate reflects the smaller (by a factor of 0.5) translational energy loss suffered by ions which have twice the translational energy of the $(M+H)^+$ ions, leading to observed relative peak shifts which are smaller (by a factor of 0.25) than those observed in the CID spectrum of the $(M+H)^+$ ion.

CID spectra of the $(M+H)^+$ ion of bombesin recorded using argon as collision gas exhibited two obvious differences from spectra of the same ion

recorded using helium. Firstly, the positions of the fragment peaks shifted markedly; average parent translational energy loss was reduced from $50 \pm 7 \text{ eV}$ with helium to $19 \pm 4 \text{ eV}$ with argon. Secondly, a shoulder on the parent peak when using helium was not present when using argon (Fig. 7). The shoulder was not present when the collision cell was evacuated. The shoulder observed with helium collision gas has an intensity which is 4–5% of the intensity of the parent peak in the absence of collision gas. On the basis of its area, the shoulder represents about 10% of the total ion current entering the collision cell. Attributing the shoulder to $(M+H)^+$ ions which have collided but have not undergone decomposition, its position corresponds to a translational energy loss of $50 \pm 20 \text{ eV}$.

Internal energy uptake Q

As implied above, the CID spectrum of the $(M+H)^+$ ion of bombesin obtained using argon as the collision gas was the same as the spectrum obtained using helium (Fig. 5). Furthermore, the intensities of the peaks relative to that of the incident $(M+H)^+$ beam were the same in each case, and, as mentioned, the optimum collision pressures were the same. We conclude that the internal energy of the $(M+H)^+$ ion following collision was the same with argon as with helium. If the scattering angle θ_i is negligible with both argon and helium, the

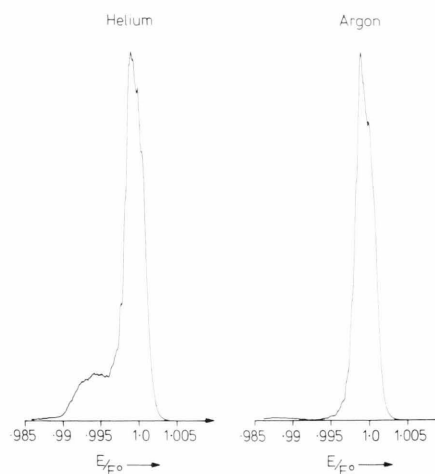


Fig. 7. Parent peak from the CID spectrum of the $(M+H)^+$ ion of bombesin recorded using helium collision gas (left hand peak) and argon collision gas (right hand peak) at the optimum collision pressure (0.1 Pa in each case).

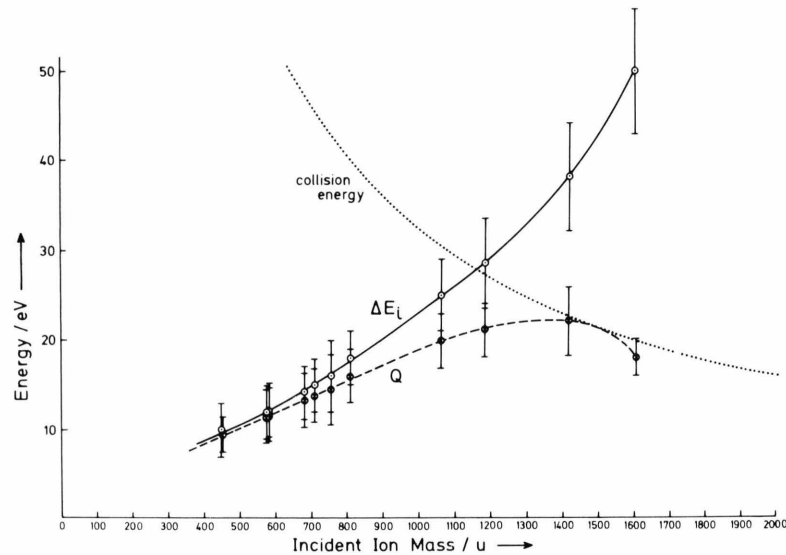


Fig. 8

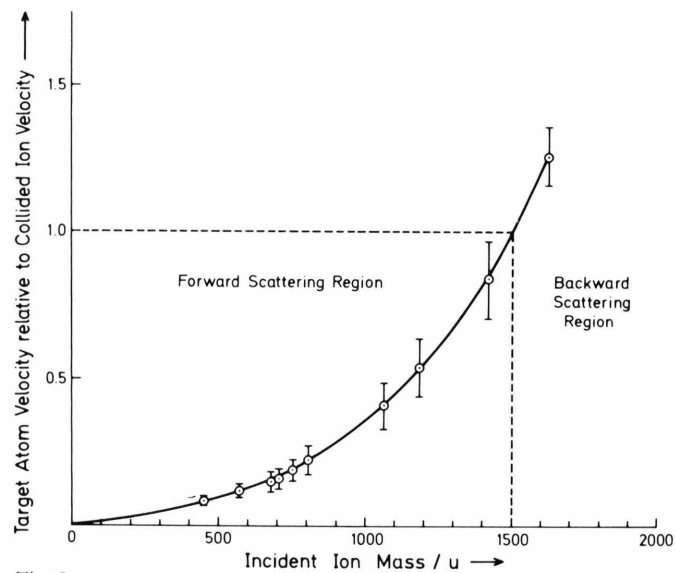


Fig. 9

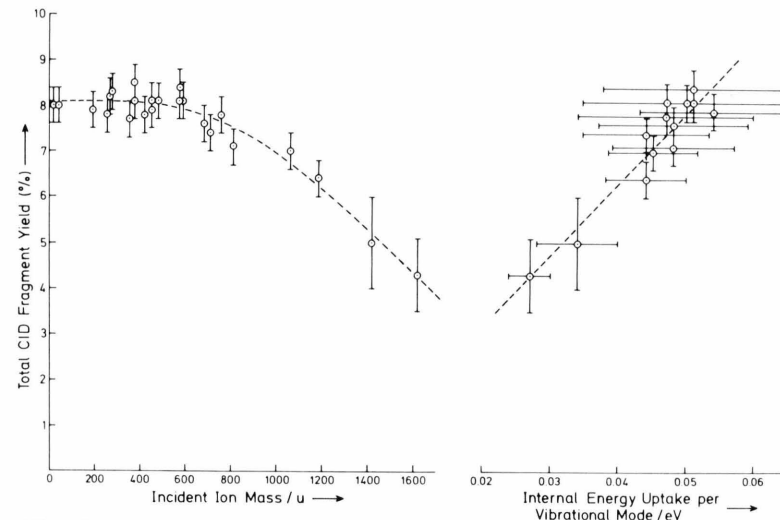


Fig. 10

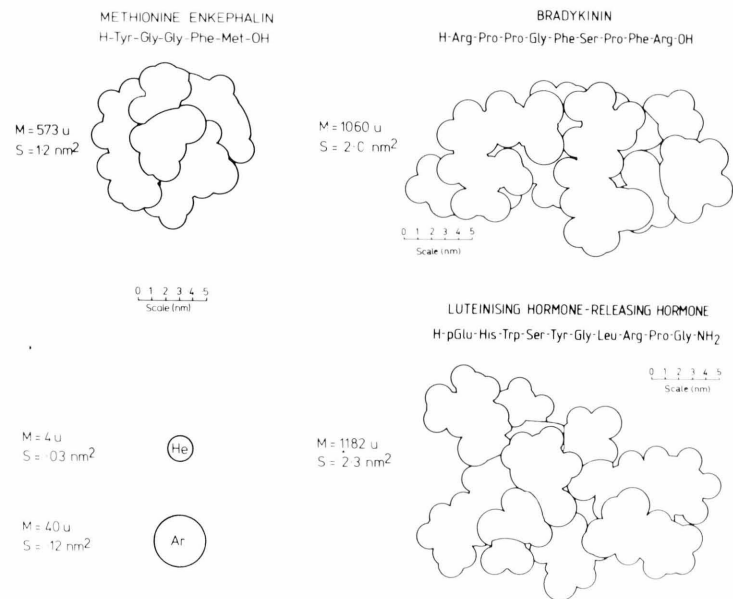


Fig. 11

internal energy uptake Q of the $(M+H)^+$ ion is 18.5 ± 2 eV with helium (calculated from $\Delta E_i = 50 \pm 7$ eV) and 18.5 ± 4 eV with argon (calculated from $\Delta E_i = 19 \pm 4$ eV). Negligible scattering angles θ_i are consistent with the results of angle-resolved measurements using small ions ($m_i \sim 100$ u) at kilo-electron volt energies, which indicate that CID spectra originate predominantly from parent ions scattered through zero or near-zero angles [17].

Comparing the CID spectra of the $(M+H)^+$ and $(M+2H)^{2+}$ ion (Figs. 5 and 6 respectively), the intensities of corresponding fragment peaks relative to that of the incident ion beam are similar. The comparisons here are between neutral losses from $(M+2H)^{2+}$ to give doubly-charged fragment ions and the losses of the same neutrals from $(M+H)^+$. The most intense fragment peak is 0.003 of the intensity of the incident ion beam with both $(M+H)^+$ and $(M+2H)^{2+}$. The internal energy uptake Q of the $(M+2H)^{2+}$ ion, calculated from $\Delta E_i = 25 \pm 15$ eV, is 21 ± 10 eV, c.f. 18.5 ± 2 eV for $(M+H)^+$.

The dependence of the internal energy uptake Q upon incident ion mass m_i is shown in Fig. 8. The translational energy loss ΔE_i and the collision energy in the centre-of-mass frame $E_{C.O.M.}$ are also shown. The points at $m_i = 1414$ u are based on measurements of the shift of the $(M+H)^+$ peak in the CID spectrum of the $(2M+H)^+$ ion of eleodoisin-related peptide [13]. The internal energy uptake Q and the translational energy loss ΔE_i fix the translational energy ΔE_a of the helium after collision (expression (2)), so that the velocity of the helium atom is known. The dependence upon incident ion mass of the ratio of the velocity of the helium atom to that of the ion m_i following collision is shown in Fig. 9.

The variation of total collected fragment ion yield with incident ion mass is shown in Fig. 10 (a). Individual fragment ion yields have been estimated from peak areas. The total collected fragment ion

yield is expressed as a percentage of the incident ion intensity based on the parent peak area. Results of measurements on m/z 16 from methane and m/z 42 from acetonitrile are included together with the results of measurements using peptide ions. There is a fall-off in total fragment ion yield with increasing ion mass, particularly above m/z 1000. In order to examine the relationship between the fall-off in total fragment ion yield and internal energy uptake Q , the total fragment ion yield has been compared with the internal energy uptake per vibrational mode. The plot of total fragment ion yield versus internal energy uptake per vibrational mode, shown in Fig. 10 (b), indicates a linear relationship with a reasonable degree of correlation between the two (correlation coefficient 0.95).

Discussion

The significance of the “optimum collision pressure”, as employed for all measurements reported here, is, we suggest, that this is the pressure at which the probability of a single collision is at its maximum. Consider that the probability distribution for different numbers of collisions is described by a Poisson distribution. The probabilities of 0, 1, 2, 3 and so on collisions are, therefore, e^{-x} , $x e^{-x}$, $\frac{1}{2} x^2 e^{-x}$, $\frac{1}{6} x^3 e^{-x}$ and so on, where x is proportional to pressure. The probability of a single collision is a maximum at $x = 1$, at which pressure $1/e$ (37%) of the ions do not collide, $1/e$ (37%) suffer one collision, $1/2e$ (18%) collide twice, $1/6e$ (6%) collide three times and so on. The “optimum collision pressure” in all our experiments represented an attenuation to between 30% and 40% of the original incident ion density. When the probability of a single collision is a maximum, the average number of collisions per ion is 1. Not all collisions, however, lead to fragment ions contributing to the CID spectrum, since the total yield of fragment ions

Fig. 8. Dependence of the translational energy loss ΔE_i suffered by the incident ion (solid curve), internal energy uptake Q (broken curve) and collision energy $E_{C.O.M.}$ in the centre-of-mass frame (dotted curve) upon incident ion mass m_i . Helium collision gas. Incident ion energy 8 keV in all cases.

Fig. 9. Dependence upon incident ion mass m_i of the ratio v_a/v_i of the velocity of the helium target atom following collision to that of the ion following collision. Velocities are in the laboratory frame. Incident ion energy 8 keV in all cases.

Fig. 10. Dependence of total CID fragment yield upon (a) incident ion mass m_i and (b) internal energy uptake per vibrational mode. Helium collision gas. Incident ion energy 8 keV in all cases.

Fig. 11. Calculated physical cross-sections S of the peptides methionine enkephalin, bradykinin and luteinising hormone-releasing hormone. Helium and argon are shown for comparison.

is always less than 10% (Fig. 1), (cf. 60–70% of the incident ion beam which has been lost). Scattering losses are probably negligible, since, with m/z 1620 and a translational energy loss ΔE_i of 50 eV (at $E_i = 8$ keV), even elastically scattered ions should pass through the electric sector. It is suggested that the remaining ion current is lost in two ways. First, a proportion of the excited parent ions do not decompose before they reach the detector or they decompose within the analyser. The shoulder on the parent ion peak m/z 1620 of bombesin (Fig. 7) supports this suggestion. Second, incident ions undergo charge transfer with the target atom [12]. The presence of singly-charged ions in the CID spectrum of the doubly-charged $[M+2H]^{2+}$ (Fig. 6) establishes that charge transfer does occur.

The bombesin ion m/z 1620 loses 50 eV of translational energy (maximum uncertainty ± 7 eV) in collision with helium at 8 keV incident energy. It follows directly that in the centre-of-mass frame back-scattering occurs, i.e. in the laboratory frame the helium atom following collision moves ahead of the ion down the instrument's flight path. This finding is demonstrated clearly by the relative magnitudes of the velocities of ion and atom after collision (Fig. 9). The incident ions of lower mass studied are forward-scattered, i.e. in the laboratory frame the helium atom is left behind by the ion. The bombesin ion m/z 1620 in collision with argon at 8 keV is also forward-scattered, as is this same ion in collision with helium at 20 keV. In considering the significance of the change from forward-scattering to back-scattering, which at 8 keV with helium occurs as the incident ion mass is raised from m/z 1400 to m/z 1600, it is important to note that the collisions are effectively "head-on". The physical cross-sections S of many of the isolated peptides studied are available from calculations [18–20]. Scale drawings of 3 of the peptides are shown in Fig. 11 together with the target atoms. The physical cross-sections S are comparable to the absolute collision cross-sections σ (Fig. 1), and are clearly much greater (30 to 100 times) than the cross-sectional area of a helium atom. Forward-scattering following a "head-on" collision corresponds to the target atom passing completely through the incident ion. Given the high axial symmetry likely for the forces involved, it is reasonable that the angle through which the atom is scattered is close to zero. Back-scattering in a "head-on"

collision means that the helium atom is incapable of passing completely through the multiatomic ion, being reflected before this can be achieved. A transition from forward-scattering to back-scattering as incident ion mass is raised implies that at a certain mass the ion and atom would not be scattered at all. That is to say, the ion and atom would remain together following collision, and their velocities in the laboratory frame would be the same (see Fig. 9). All of the collision energy in the centre-of-mass would be taken up as internal energy, so that the internal energy plot should touch the collision energy plot as shown in Figure 8.

It can be seen from Fig. 8 that, with helium and an incident ion energy of 8 keV, the internal energy uptake Q increases steadily with increasing ion mass m_i up to about mass 1400 u. The collision energy $E_{C.O.M.}$ falls as approximately $1/m_i$ over this same range, so that the *proportion* of the available collision energy converted to internal energy rises very sharply at the lower masses and then more gradually at higher masses as it begins to approach 1. It appears that the proportion of the collision energy converted to internal energy begins to drop again, once the change from forward-scattering to backward-scattering has occurred. The picture which emerges in the centre-of-mass frame is that the interaction between the ion and helium becomes steadily greater as the size of the ion increases from 400 u up towards 1400 u. The atom continues to penetrate the ion completely, but the proportion of their momentum lost by ion and atom rises as the length of the interaction region (the "thickness" of the ion) becomes larger. Eventually, both ion and atom are brought to a standstill, at which point it may be reasonable to think of the atom being trapped within the ion. With 8 keV ions incident on helium, this happens at about mass 1500 u. As the ion mass and hence the length of the interaction region is increased further, the ion and atom begin to rebound from each other, and not all of the collision energy is converted to internal energy. If the collision energy $E_{C.O.M.}$ is raised significantly either by replacing helium with argon or by increasing the incident ion energy to 16 keV (as with $(M+2H)^{2+}$ from bombesin), or 20 keV (as in the measurement with $(M+H)^+$ from bombesin), the much greater momentum associated with the collision means that at masses up to 1600 u forward-scattering always occurs. That is to say, the argon

atom at the 8 keV ion energy or the helium at 16 keV or 20 keV penetrate right through the ion.

The implication for collision-induced decomposition as a method of analysis for macromolecules is that the mass of the target atom and the incident ion energy should be "tuned" to the incident ion mass. With m/z 1620 from bombesin, helium and argon have been found to deposit comparable amounts of internal energy within the ion. At higher masses, the internal energy taken up by an ion in collision with helium must fall because the collision energy drops. Whereas with argon, if the trends discovered for helium apply, the proportion of the collision energy converted to internal energy will rise on moving to moderately higher ion masses and the internal energy uptake itself will rise. It is pointed out that, for forward-scattering of a given incident ion and a given target atom, there is no evidence in the results presented here of the internal energy uptake increasing as the incident ion energy is raised. Of fundamental interest is the prediction that, following collision between an incident ion with keV translational energy and a stationary atom,

the ion and atom will not separate if their masses are in the proper ratio. The ion and atom would in effect constitute a complex with keV translational energy and internal excitation energy equal to the collision energy. We are actively seeking to test this prediction. In the case of helium, the interaction between atom and ion is unlikely to induce chemical reaction. If, however, helium were replaced by a potentially reactive species such as D₂, the possibility opens up of chemical reaction within an isolated energised complex of known composition, with known internal energy, with a lifetime fixed by the flight-time prior to entering the analyser and with the ready facility for analysis of the reaction products.

Acknowledgements

We are pleased to acknowledge financial support under the Australian Research Grants Scheme. Valuable discussions with Dr. J. R. Christie, Dr. S. Nordholm, and Dr. A. D. Rae are gratefully acknowledged.

- [1] H. D. Beckey, *Int. J. Mass Spectrom. Ion Phys.* **2**, 500 (1969).
- [2] H. D. Beckey and H.-R. Schulten, *Angew. Chem. Int. Ed.* **14**, 403 (1975).
- [3] P. G. Cullis, G. M. Neumann, D. E. Rogers, and P. J. Derrick, *Adv. Mass Spectrom.* **8**, 1729 (1980).
- [4] T. Matsuo, H. Matsuda, I. Katakuse, Y. Shimonishi, Y. Maruyama, T. Higuchi, and E. Kubota, *Anal. Chem.* **53**, 416 (1981).
- [5] P. J. Todd, D. C. McGilvery, M. A. Baldwin, and F. W. McLafferty, in "Tandem Mass Spectrometry", ed. F. W. McLafferty, John Wiley and Sons, New York 1983, p. 271.
- [6] K. Levsen, *Fundamental Aspects of Organic Mass Spectrometry*, Verlag Chemie, Weinheim 1978.
- [7] P. J. Todd and F. W. McLafferty, in "Tandem Mass Spectrometry", ed. F. W. McLafferty, John Wiley and Sons, New York 1983, p. 149.
- [8] A. G. Craig and P. J. Derrick, unpublished results.
- [9] G. M. Neumann and P. J. Derrick, *Org. Mass Spectrom.*, in press.
- [10] H. D. Beckey, E. Hilt, and H.-R. Schulten, *J. Phys. E: Sci. Instrum.* **6**, 1043 (1973).
- [11] G. M. Neumann, P. G. Cullis, and P. J. Derrick, *Z. Naturforsch.* **35a**, 1090 (1980).
- [12] R. G. Cooks, J. H. Beynon, R. M. Caprioli, and G. R. Lester, *Metastable Ions*, Elsevier Sci. Publ. Co., Amsterdam 1973.
- [13] P. H. Dawson, *Int. J. Mass Spectrom. Ion Phys.* **43**, 195 (1982).
- [14] W.-F. Sun and P. H. Dawson, *Org. Mass Spectrom.* **18**, 396 (1983).
- [15] (a) G. M. Neumann, Ph.D. Thesis, La Trobe University, Victoria, Australia, 1983; (b) G. M. Neumann and P. J. Derrick, *Aust. J. Chem.*, submitted for publication; (c) P. J. Derrick and G. M. Neumann, "Tandem Mass Spectrometry", ed. F. W. McLafferty, John Wiley and Sons, New York 1983, p. 223.
- [16] R. Weber and K. Levsen, *Org. Mass Spectrom.* **7**, 314 (1980).
- [17] R. G. Cooks, private communication (1983).
- [18] Y. Isogai, G. Nemethy, and H. Scheraga, *Proc. Nat. Acad. Sci. USA* **74**, 414 (1977).
- [19] G. S. Galaktionov, S. A. Sherman, M. D. Shenderovich, G. V. Nikiforovich, and V. I. Leonova, *Biorg. Khim.* **3**, 1190 (1977).
- [20] (a) F. A. Momany, *J. Amer. Chem. Soc.* **98**, 2990 (1976). – (b) F. A. Momany, *J. Amer. Chem. Soc.* **98**, 2996 (1976).